SCANNING ELECTRON MICROSCOPY FOR THE CHARACTERIZATION OF A CERAMIC MEMBRANE COMPOSED OF $LaFeO_3$-CeO_2 AND La_2O_3-Al_2O_3

G. Rodríguez[a], L. C. Maldonado[a], T. Humbría [a], J. Anzola[a], Y. Diaz [a], J. L. Brito[a,b], R. S. Del Toro [a]*

[a] Laboratorio de Físico Química de Superficies, Centro de Química "Dr Gabriel Chuchani", Instituto Venezolano de Investigaciones Científicas (IVIC), Caracas 1020-A, Venezuela.
[b] Universidad Regional Amazónica IKIAM, Tena, Ecuador

*Corresponding author, Email: raqueldeltoro.ivic@gmail.com, rdeltoro@correo.ivic.gob.ve, phone: +58 (212) 504.3082/1346, Fax.: 5041426

Received: 15-07-2024 Accepted: 12-09-2024
Published: 27-03-2025

ABSTRACT
The chemical composition, crystalline structure and microstructure of ceramic membranes play an important role in their mechanical properties, thermal stability, permeation and catalytic behavior. In the present work, a mixed ceramic membrane with potential application in catalysis was prepared and characterized. The ceramic membrane was made of two layers of ceramic oxides with a dense and porous structure. The dense layer was prepared with a solid composite based on $LaFeO_3$ of perovskite-like structure and CeO_2. The porous layer was prepared with a La_2O_3-Al_2O_3 composite oxide. The constituent powders and the ceramic membrane were characterized by XRD, SEM-XEDS, BSC and nitrogen physisorption. The microstructure results showed an adequate compaction of the dense and porous ceramic powders, with a grain consolidation boundary zone of the two ceramic phases up to a certain depth (< 200 μm) and relative roughness without fracture between the two ceramic oxide layers.

Keywords: ceramic membrane, La_2O_3-Al_2O_3, $LaFeO_3$, CeO_2, SEM

MICROSCOPÍA ELECTRÓNICA DE BARRIDO PARA LA CARACTERIZACIÓN DE UNA MEMBRANA CERÁMICA COMPUESTA DE $LaFeO_3$-CeO_2 Y La_2O_3-Al_2O_3

RESUMEN
La composición química, estructura cristalina y la microestructura de las membranas cerámicas juegan un rol importante en sus propiedades mecánicas, estabilidad térmica, permeación y comportamiento catalítico. A través del presente trabajo, se preparó y caracterizó una membrana cerámica mixta de potencial aplicación en catálisis. La membrana cerámica se conformó con dos capas de óxidos cerámicos de estructura densa y porosa. La capa densa fue preparada con un sólido compósito a base de $LaFeO_3$ de estructura tipo perovskita y CeO_2. Mientras que la capa porosa fue preparada con un óxido compuesto La_2O_3-Al_2O_3. Se caracterizaron los polvos constituyentes y la membrana cerámica por XRD, SEM-XEDS, BSC y fisisorción de nitrógeno. Los resultados de la microestructura mostraron una adecuada compactación de los polvos cerámicos denso y poroso, con una zona frontera de consolidación de granos de las dos fases cerámicas hasta cierta profundidad (< 200 μm) y relativa rugosidad sin fractura entre las dos capas de óxidos cerámicos.

Palabras claves: membrana cerámica, La_2O_3-Al_2O_3, $LaFeO_3$, CeO_2, SEM

INTRODUCTION

Membranes are described as a physical barrier that separates two phases, and through which the selective transport of chemical species occurs [1]. A catalytic membrane is a device that serves to simultaneously carry out a chemical reaction and a separation. The membrane itself can act as a catalyst or the catalyst can be impregnated into the membrane [2].

Moreover, the reactor containing the catalytic membrane can be bifunctional and two complementary reactions can occur on different sides of the membrane, the reaction products on one side acting as reactants on the other side,

while the endothermicity of one reaction is compensated by the exothermicity on the other [2].

In turn, inorganic membranes, which include ceramics, favor applications under severe conditions such as high temperatures, aggressive mixtures (chemical, mechanical, microbiological) and high pressures. Contrary to polymeric membranes which are unstable under such conditions. In terms of composition, ceramic membranes can be porous, dense and mixed sandwich membranes, which are composed of porous and dense ceramic layers (see Figure 1) [3,4].

Initially, ceramic membranes were developed for uranium enrichment and were also used in wastewater treatment. In recent years, their applications have increased in different sectors, such as biotechnology, pharmaceuticals, food and beverages. As well as in the chemical, petrochemical, microelectronic and automotive sectors, among others [5].

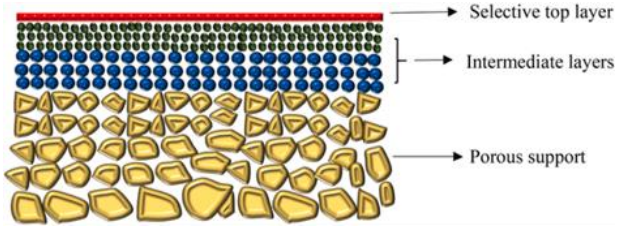

Figure 1. Schematic figure of the different layers and microstructure of a mixed ceramic membrane, taken from reference [1].

An interesting class of materials that possess high oxygen conductivity and are expected to meet the requirements of catalytic membranes are perovskite (ABO_3) and derivatives, given their characteristics as mixed ionic-electronic conducting metal oxides. Although some of the properties of these solids have been studied in the exchange and transport of oxygen [6-7], their catalytic activity for the production and purification of green or blue hydrogen opens up a wide field of research in the development of this type of inorganic membranes.

However, it is important to improve the thermal stability and ionic/electronic conduction properties of $LaFeO_3$ perovskite oxide membranes. For this purpose, cerium (Ce) has been used as an interesting structural dopant. Previous studies of the group [8-9] have contributed to the compression of this composite material and to the optimization of the synthesis protocols for obtaining the precursor powders and the preparation of dense $LaFeO_3$-CeO_2-based membranes. In this sense, Bermúdez [8] developed sintered discs for application in sensors based on $La_{1-x}Ce_xFeO_3$ and CeO_2, using the protocol of pressing the powder and sintering at 1373.15 K. Scanning electron microscopy analysis of the sensors indicated the absence of fractures in the ceramic device with an acceptable level of aggregation of the material grains. The sensitivity of the $La_{1-x}Ce_xFeO_3$ - CeO_2 (x=0.1 and 0.3) based sensor was evaluated resulting in high detection of N_2 gas, and to a lesser extent CO_2 and CO_2/N_2 gases. Ce doping substantially improved the sensitivity of the sensor, showing intrinsic conductivity, which is dependent on temperature, gas type (reducing or oxidizing) and Ce composition. Similarly, Maldonado *et al.* [9] prepared and characterized $LaFeO_3$-CeO_2 ceramic membranes, addressing the study of thermal and chemical stability under catalytic oxidation working gases. The results indicated that the chemical and thermal stability of $LaFeO_3$-CeO_2 composite membranes was maintained under oxidizing and inert gases at temperatures (773.15-1073.15) K. On the other hand, in the presence of a reducing CH_4 environment, the stability of the dense membrane was achieved up to below 873.15 K. Above this temperature, the irreversible transformation of the metal oxides to the reduced metal state and the formation of amorphous carbonaceous species and carbon nanotubes were observed. On the other hand, in relation to the porous support, alumina is considered as a suitable metal oxide, very versatile and widely used in catalysis and ceramic membrane applications. However, it is also important to ensure its phase stability at elevated temperatures. In this regard, Ersoy *et al* [10] studied the effect of lanthanum oxide addition on the thermal stability of alumina gels. They

found that the addition of La_2O_3 at different concentrations improved the thermal stability of the material with respect to undoped γ-alumina. The addition of lanthanum oxide helped to keep the pore size and pore size distribution small even at sintering temperatures of 1473.15 K. The thermal stability of γ-alumina was attributed to the presence of lanthanum oxide on its surface, which reduced the possibility of nucleation, delaying the phase transformation from γ-alumina to α-alumina at high temperatures [10]. However, its incorporation must be done at low concentrations to avoid problems of increased acidity in the support. [11-12]. Thus, it is expected that the incorporation of oxides containing rare earth cations such as La_2O_3 on the alumina support could improve and thermally stabilize alumina, improve its structural stability [13-14], and be useful in the configuration of ceramic membranes and their application in catalysis. It should be noted that, scanning electron microscopy (SEM) is a technique widely used by membrane manufacturers and researchers in the field, to measure the thickness of deposited films, track structural and morphological changes of their constituent materials, examine their microstructure, grain boundaries of the deposited species, monitor defects, cracks, among others [5]. However, there are interesting stability improvements of alumina powders when forming mixed supports with rare earth oxides such as La_2O_3, CeO_2 [10-12, 15]. To the best of our knowledge, their forming into a compact porous La_2O_3-Al_2O_3 membrane-like porous structure has not yet been addressed. Furthermore, the preparation procedure presented in this study is not known to have been used for the development of a mixed $LaFeO_3$-CeO_2/La_2O_3-Al_2O_3 ceramic membrane. Therefore, the present work, contemplates the preparation and characterization of a mixed ceramic membrane, composed of a porous layer of La_2O_3-Al_2O_3 and a dense layer based on $LaFeO_3$ and CeO_2.

MATERIALS AND METHODS

Alumina Synthesis

For the synthesis of the support, the boehmite hydrolysis method was used, for which an amount of aluminium nitrate $Al(NO_3)_3$-$9H_2O$ was dissolved in distilled water in a heating plate under agitation at 353.15 K. It was then hydrolyzed by adding ammonia until pH=8 was adjusted. Then, it was separated the aluminium hydrate from the solution by vacuum filtration and washed in triplicate with distilled water. The solid was acidified by adding HNO_3 solution, the colloidal salt was observed to form, which was then heated at 373.15 K to obtain the gel. The gel was evaporated on a heating plate and dried in an oven for 24 hours and calcined at 923.15 K in a muffle.

Preparation of the La_2O_3-Al_2O_3 composite

La_2O_3-Al_2O_3 composite oxide powder was prepared by incipient impregnation of the synthesized alumina with an aqueous lanthanum nitrate solution to achieve 3% w/w La over Al_2O_3. Subsequently, it was dried in an oven at 353.15 K for 24 hours and then calcined at 873.15 K in a muffle.

Synthesis of the $LaFeO_3$ - CeO_2 composite

The synthesis of the composite oxide powder $LaFeO_3$ - CeO_2 was carried out using the sol gel-citrate method, for which stoichiometric amounts of La_2O_3, $Fe(NO_3)_3$. $9H_2O$ and $CeCl_3$ in a molar ratio of citric acid (CA) to total metal ions CA/(La + Fe + Ce)= 1, the first of these solids was dissolved in concentrated nitric acid, with subsequent addition of the other salts, then citric acid was added, stirring and heating at 353.15 K until the gel was obtained, and finally the solvent was evaporated. The obtained gel was dried for 24 hours and the obtained xerogel was calcined at 1073.15 K for 4 h.

Preparation of the mixed membrane

The dry powder of the La_2O_3-Al_2O_3 composite was prepared, by gentle grinding in a mortar and sieving until an average grain size of <45µm was obtained. It was then mixed with 2 % w/w polyvinyl alcohol binder (10 % in aqueous solution) and dried at 353.15 K for 30 min. The sample was then placed in a steel die-type mold and pressed uniaxially into a cylindrical sheet (ceramic disc) using a hydraulic press at a pressure of 12.5 MPa. Subsequently, a measured amount of dry powder of $LaFeO_3$ - CeO_2 composite was incorporated and distributed grain size between (45 - 90) µm premixed with the binder. A second uniaxial pressing was performed and the raw ceramic disc was generated by compacting two layers of ceramic oxides. The dimensions of the latter were approximately 10 mm diameter x 1 mm thick. Finally, the ceramic disc was removed from the mold, and sintered in static air at temperatures of 1373.15 K

Characterization of the precursor powders and membranes

The La_2O_3-Al_2O_3 and $LaFeO_3$-CeO_2 composite powders as well as the mixed membrane were characterized using X-ray diffraction (XRD), N_2 physisorption textural analysis and SEM-EDX scanning electron microscopy. Operational details are given below.

X-ray diffraction

Diffraction patterns of the precursor powders and membranes were performed on a SIEMENS D5005 diffractometer using Cu-Kα radiation (λ=1.5456 Å) and Ni filter, these were evaluated between (20-80) °/ 2θ with a step speed of 0.04 °/s. Phase identification was performed with the JCPDS database.

Textural analysis by N_2 physisorption

Textural analysis of the synthesized materials was performed with an automatic analyzer Micromeritics-ASAP 2010 at 77 K. The specific surface areas were calculated by the Brunauer-Emmett-Teller (BET) method, the pore volume (Vp) was determined by adsorption at a relative pressure of 0.98 and the pore size distribution by the Barret-Joyner-Halenda (BJH) method.

Scanning electron microscopy (SEM)

A JEOL model JSM-6390 was used. To determine the chemical composition, an electron microscope coupled to an OXFORD Instruments model 7582 X-ray energy dispersive microanalyzer (XEDS) was used. The micrographs were taken with an LFD (Large Field Detector) detector.

RESULTS AND DISCUSSION

Characterization of La_2O_3-Al_2O_3 alumina and oxide composite powders

Figure 2 shows the X-ray diffractograms for alumina powder (Fig. 2a) and La_2O_3-Al_2O_3 (Fig. 2b). In which the γ-Al_2O_3 phase (JCPDS file 29-0063.) present in both solids was identified. No evidence of modification of the γ-Al_2O_3 structure after incorporation of La_2O_3. No signals due to lanthanum oxide were observed, indicating a good dispersion on the support.

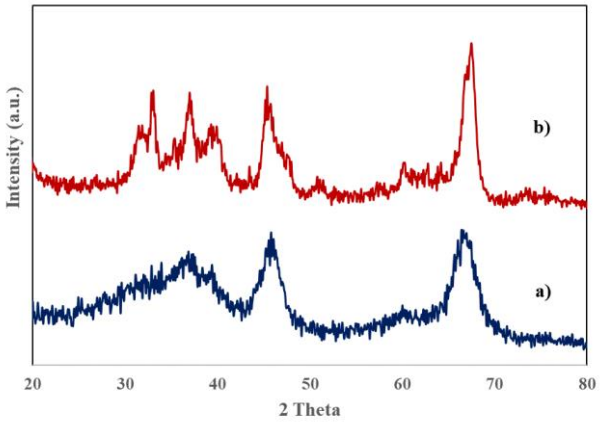

Figure 2. X-ray powder diffractogram: (a) alumina obtained from the hydrolysis of boehmite, (b) La_2O_3-Al_2O_3 composite oxide

This is consistent with the results of the XEDS elemental mapping analysis (Fig. 3) of the La_2O_3-Al_2O_3-based porous solid, which confirmed the presence of lanthanum in the solid and at 3 % La in alumina, a homogeneous dispersion of La was achieved along the grain at a scale of less than 2.5 µm. No evidence of agglomeration of this element (in its corresponding oxide phase La_2O_3), in relation to the aluminium mostly present in this Al_2O_3-based system.

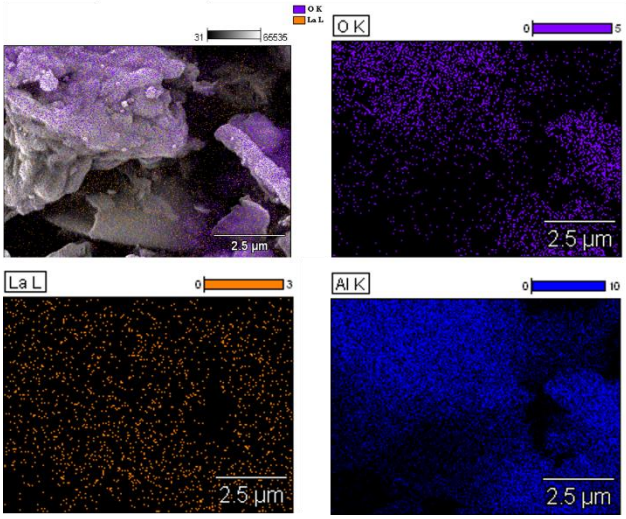

Figure 3. Elemental mapping of La_2O_3-Al_2O_3 oxide powder

Regarding the morphology of the alumina grains, before and after the incorporation of La_2O_3, an amorphous characteristic of particular agglomerates of irregular shape and size in the appearance of a cluster of random flakes was observed for the initial phase of the γ-alumina (Fig. 4a). For its part, the La_2O_3-Al_2O_3 composite oxide (Fig. 4b), although it maintained the amorphous morphology of particle aggregates and relatively similar grain size as the precursor alumina, differed in the smoothing of its surface (flaking). In addition, it revealed a coating of tiny crater-type depressions, of the submicrometer order, apparently not very deep.

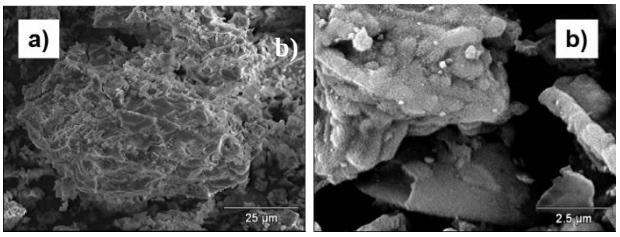

Figure 4. SEM image of powder: a) Al_2O_3, b) Composite oxide La_2O_3-Al_2O_3

The nitrogen adsorption-desorption isotherms of pure and lanthanum-impregnated alumina powders are presented below. Figure 5 shows type IV isotherms for the two materials, which are characteristic of mesoporous solids according to the IUPAC classification [16, 17]. The values of area, pore volume and pore diameter of each solid are shown in Table I. Similar behavior was reported by Ersoy *et al.* [18], where they found that the addition of 1 to 5 % lanthanum oxide in γ-Al_2O_3 decreased the surface area in the same way as observed in this case, which was not a significant drop. In this regard, Ismagilov *et al.* [19], reported that the incipient impregnation method is more efficient compared to the introduction of lanthanum into granular aluminium hydroxides. Additionally, they found that the doping of alumina with cerium provides a minor effect on thermal stability with respect to lanthanum incorporation.

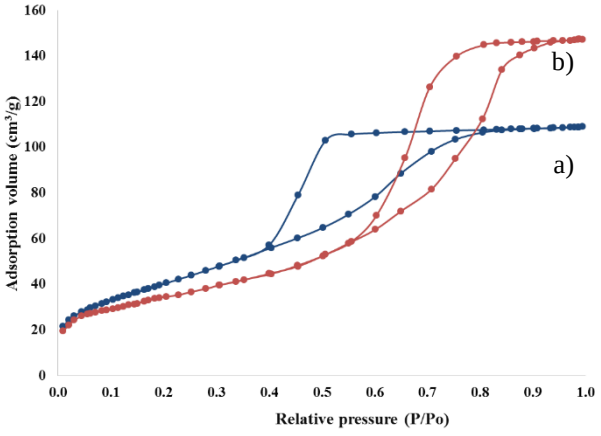

Figure 5. Adsorption isotherms: (a) Al_2O_3 (b) La_2O_3-Al_2O_3 composite oxide

On the other hand, a hysteresis loop shift was observed upon incorporation of lanthanum oxide into alumina. The hysteresis loop shifted from H2(b) to H2(b) with a shifted hysteresis loop at intermediate relative pressures in the P/Po 0.5-0.9 partial pressure region upon incorporation of lanthanum oxide into alumina. In general, the H2 hysteresis loop is characteristic of structures formed by interconnected, less ordered quasi-cylindrical mesoporous of different shape and size, which have been reported in oxides from inorganic gels [20, 17].

The fact that both materials share this characteristic is to be expected since they are made of the same base or starting material, i.e. alumina. However, the La_2O_3-Al_2O_3 composite system had a hysteresis of H2(b), attributed to an ink-bottle pore shape. This informs us of a blocking effect of the desorption pore in the solid, with the incorporation of lanthanum oxide into the alumina. However, the drop in specific surface area of the alumina support (Table I) was not significant (14.2 %). Indeed, the relative improvement of the pore volume (Table I), and the enlarged pore size distribution with a trend towards larger pore sizes (Fig. 6), within the mesoporous range, could indicate a contribution of lanthanum oxide to this new porosity of the solid.

In this vein, Fig. 6 a-b presents the pore diameter distribution of the Al_2O_3 and La_2O_3-Al_2O_3 composite solids, which presented relatively narrow average pore diameter distributions, with a pore diameter centered at 3.6 nm for the Al_2O_3 sample and at 3.2 and 5.8 nm for the La_2O_3-Al_2O_3 composite sample, the latter showing a bimodal pore size distribution.

Table I. Textural characteristics of alumina-based powders

Sample / Powder	S_{BET}[a] ($m^2 \cdot g^{-1}$)	Pore volume[b] ($cm^3 \cdot g^{-1}$)	Pore size[c] (nm)
Al_2O_3	147.81	0.18	4.56
La_2O_3-Al_2O_3	126.84	0.23	7.36

[a]S_{BET}: Surface specific area determined by BET method.
[b]Average pore volume.
[C]: Average pore size by D_{BJH} method.

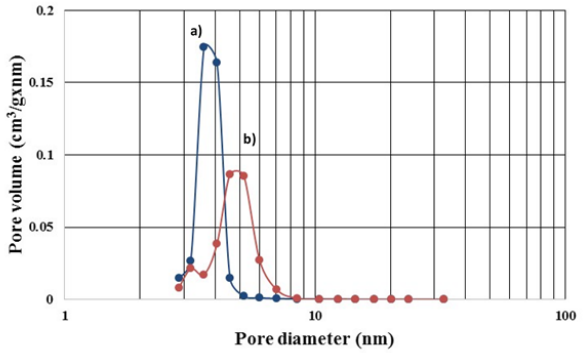

Figure 6. Pore diameter distribution of a) Al_2O_3, b) composite La_2O_3-Al_2O_3.

Characterization of perovskite metal oxides

In relation to the dense ceramic system, Figure 7 shows the nitrogen adsorption-desorption isotherm of the $LaFeO_3$-CeO_2 composite oxide. It can be classified as type II for a macroporous or non-porous material [16-17]. This result is consistent with low surface area values of 2.03 m^2/g and pore volume of 0.01 cm^3/g typical of dense materials.

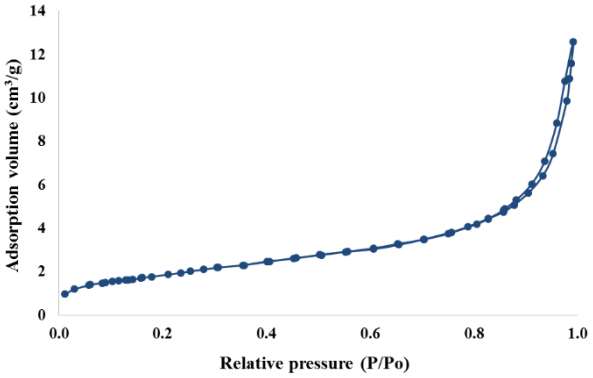

Figure 7. N_2 adsorption-desorption isotherm for the composite oxide $LaFeO_3$-CeO_2

Figure 8 shows the diffractograms of the $LaFeO_3$-CeO_2 composite oxide. The formation of the lanthanum ferrite of perovskite structure, $LaFeO_3$ (PCPDS file 75-0541) as well as the second phase due to CeO_2 (PCPDS file 75-0390) was observed. Additionally, a slight shift of the reflections of the perovskite-like oxide phase with respect

to the pattern was evidenced. This could be associated with relative cerium doping in its crystal lattice, leading to a partially Ce-substituted $La_{1-x}Ce_xFeO_{3-\delta}$ structure. A partial substitution of the A cation in the ABO_3 structure of the perovskite-like oxide is possible, due to the smaller Ce^{+3} ion size (r = 1.01 Å) compared to the La^{+3} ion (r = 1.15 Å). Such a fact would cause a contraction in the size of the perovskite oxide crystal lattice and consequent shift in the diffraction pattern.

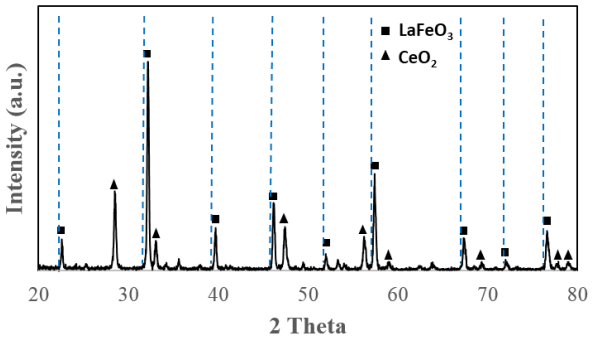

Figure 8. X-ray powder diffractogram of the composite oxide $LaFeO_3$-CeO_2

Characterization of $LaFeO_3$-CeO_2/La_2O_3-Al_2O_3 composite ceramic membrane

Below is the SEM image of the mixed ceramic membrane obtained on the flat surface of the sintered disc, on the face (of the disc) with $LaFeO_3$-CeO_2 composite oxide ceramic layer (Figure 9). A regular, flattened and fracture-free microstructure was observed in the micrographs. Also, the compaction of the irregularly shaped grains of different grain sizes formed a medium sintering level surface (Fig. 9b). This is consistent with the moderate compaction heat treatment used in the present study, which was gentler than conventional preparation conditions (>1673.15 K) to achieve complete sintering of the perovskite-like oxide particles [21].

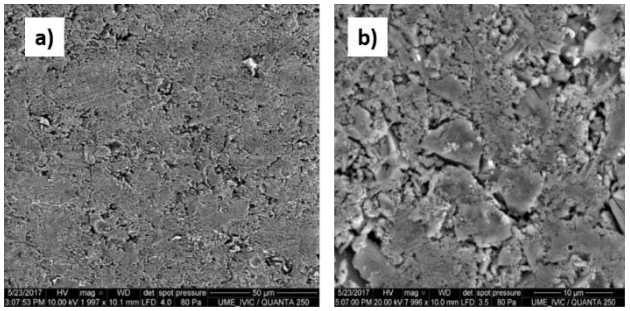

Figure 9. SEM images of the mixed ceramic membrane of the $LaFeO_3$-CeO_2 ceramic system side, a) 50 µm (approx. 2000X), b) 10 µm (approx. 8000X)

X-Ray Energy Dispersive Spectroscopy (XEDS) analysis confirmed the presence of the expected elements in the $LaFeO_3$-CeO_2 ceramic composite (Figure 10a). With weight percentages of constituent elements La, Ce, Fe and O in the order of the expected (result not included). Similarly, XEDS analysis of the La_2O_3-Al_2O_3 ceramic (Fig. 10b) corroborated an elemental composition of La, Al and O, within the weight percentages estimated for the material (result not included).

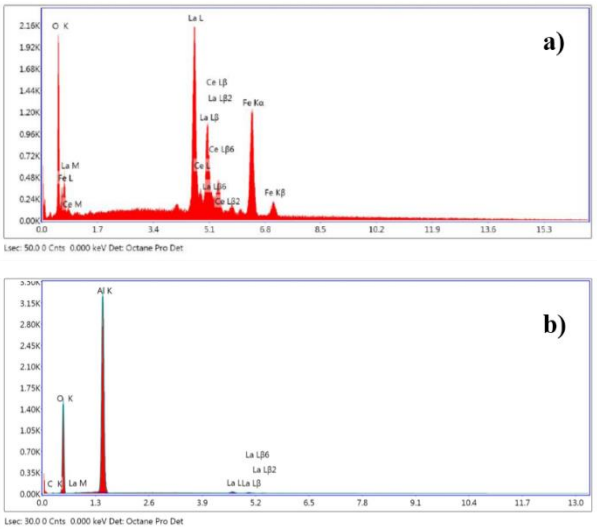

Figure 10. XEDS spectrum of the mixed ceramic membrane: a) $LaFeO_3$-CeO_2 ceramic system side; b) La_2O_3-Al_2O_3 ceramic system side.

Figure 11 corresponds to the micrograph of the membrane obtained on the surface of the La_2O_3-Al_2O_3 ceramic layered (disc) face. In which a relatively regular

microstructure was observed along the surface and moderate compaction and sintering of grains of varied shape and size. With the presence of marked surface roughness at the grain boundaries.

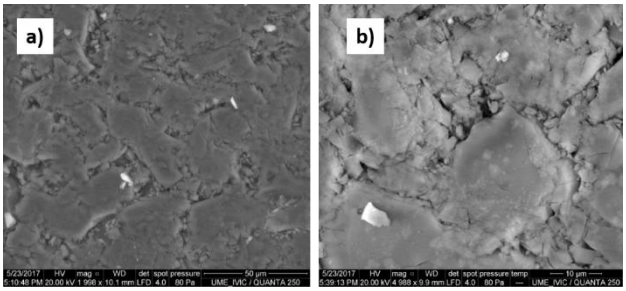

Figure 11. SEM images of the mixed ceramic membrane on the La_2O_3-Al_2O_3 side of the ceramic system (a) 50 µm (2000X), b)10 µm (5000X)

Regarding the thickness of the mixed $LaFeO_3$-CeO_2/La_2O_3-Al_2O_3 membrane, the micrograph of that area of the membrane (Figure 12) confirmed a value close to the expected one. Wear was observed in the porous layer of La_2O_3-Al_2O_3 due to handling during analysis. The percentage layer thickness ratio was 44:56 for the dense: porous system respectively. Overall, good layer compaction of the two ceramic oxides was observed at disc depth. Suggesting that the cold pressing method and sintering conditions of the mixed membrane were suitable, at a moderate level, for thin disc forming and confining.

At higher magnification, in the border zone of the dense: porous layers (Figure 13), the SEM images showed the morphology of the mixed membrane at the contact interface of the solids. It was evident that the compaction was adequate and with a boundary zone, in which grains of both ceramic systems are interlocked up to a certain limit (< 200 µm), without fractures between the ceramic layers.

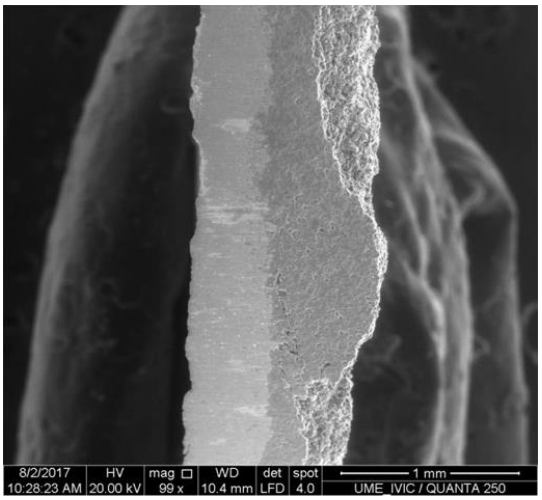

Figure 12. SEM image of the mixed ceramic membrane $LaFeO_3$-CeO_2/La_2O_3-Al_2O_3 (1mm,99X), left side of membrane: $LaFeO_3$-CeO_2 and right side: La_2O_3-Al_2O_3.

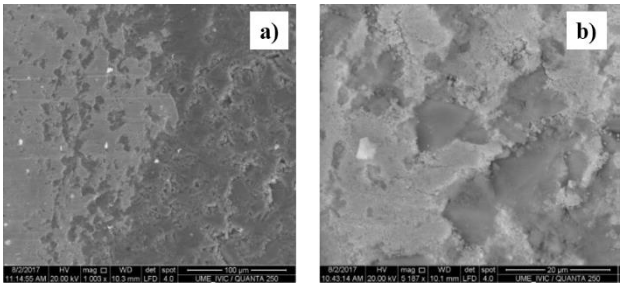

Figure 13. SEM images of the $LaFeO_3$-CeO_2/La_2O_3-Al_2O_3 mixed ceramic membrane: a) 100 µm, 1000X, b) 20 µm, 5000X

The backscattered electron contrast technique (Figure 14) allowed to distinguish more precisely the constituent phases of the solid-solid interface of the mixed membrane. On the one hand, the $LaFeO_3$-CeO_2 layer was observed bright due to higher atomic number of its constituent elements and amount of backscattered electrons. Whereas, the La_2O_3-Al_2O_3 layer was opaque due to the lower atomic number. Therefore, the signal will depend on a combination of the average atomic number and the density of the ceramic. Thus, the backscattered electron imaging provided excellent discrimination of the constituent phases of the sintered ceramic disc under study even at low voltages [22]. The $LaFeO_3$-CeO_2 phase was able to penetrate a minimal extent of the La_2O_3-Al_2O_3 porous system, without

causing total mixing of the two ceramic phases or phase impurities. This is explained by the forming procedure of the ceramic bilayer, in which grains of the $LaFeO_3$-CeO_2 composite oxide powder were deposited on the compacted La_2O_3-Al_2O_3 disc in the process of forming the mixed disc prior to pressing and sintering.

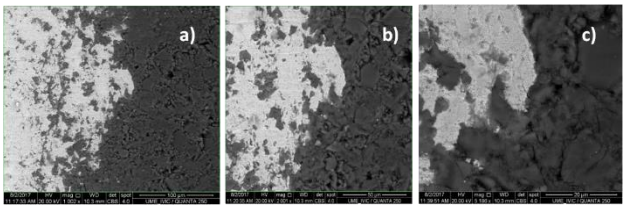

Figure 14. Backscattered electron images of the $LaFeO_3$-CeO_2/La_2O_3-Al_2O_3 mixed ceramic membrane: a) 100 µm, 1000X; b) 50 µm, 2000X; c) 20 µm, 5000X.

CONCLUSIONS

The study allowed the development of a two-phase mixed membrane composed of a novel $LaFeO_3$-CeO_2/La_2O_3-Al_2O_3 ceramic system. The morphological analysis by SEM-XEDS and BSC of the mixed membrane showed moderate grain compaction on both sides of the ceramic disc and intergranular phase characteristics at the solid (dense) - solid (porous) interface, in accordance with the type of procedure proposed for layer formation in the mixed membrane and moderate sintering temperature.

ACKNOWLEDGEMENT

The authors would like to thank the Electron Microscopy Unit (UME) of the Chemistry Centre, IVIC and Myloa Morgado for the SEM-XEDS and BSC analysis.

We would also like to thank Liz Cubillán from the Applied Chemistry Laboratory for her support in the optimization of the molding and compaction of the ceramic disc under study.

REFERENCES

[1] Sandhya Rani S.L., Kumar R.V. (2021) “Insights on applications of low-cost ceramic membranes in wastewater treatment: A mini-review” Case Studies, *Chem. Environ. Eng.* 4: 100149.

[2] Zaman J., Chakma A., (1994), “Review, Inorganic membrane reactors”, *J. Membr. Sci.* 92: 1-28.

[3] Rostrup N. (1984) “Catalysis, Science and Technology”, Berlin, Springer.

[4] Juste E, Julian A, Etchegoyen E, Geffroy P, Chartier T, Richet N, Del gallo P. (2008) *J. Mem. Sci.* 319: 185-191.

[5] Mallada R., Menéndez M. (2008) “Inorganic membranes. Synthesis, characterization and applications” Amsterdam, Elsevier, pp. 177-189.

[6] Liu, Y., Tan X., Li K., (2006) “Mixed conducting ceramics for catalytic membrane processing”, *Catal. Rev.* 48: 145-198.

[7] Chroneos A., Vovk R.V., Goulatis I.L., Goulatis L.I., (2010), “Review oxygen transport in perovskite and related oxides: a brief review”, *J. Alloys Compd.* 494: 190-195.

[8] Gabriela Bermúdez (2015) “Síntesis vía sol-gel de un óxido de La-Ce-Fe tipo perovskita para su estudio como sensor de gases”, Bachelor thesis, Universidad Central de Venezuela, Facultad de Ciencias, Escuela de Química.

[9] Maldonado L., Tosta M., Díaz Y., Brito J, Del Toro R., (2019) “Estudio de la estabilidad de membranas cerámicas catalíticas de $La_{0,7}Ce_{0,3}FeO_{3-x}$ (LCFO)”, *Catálisis* 8: 55-62.

[10] Ersoy B, Gunay V. (2004). “Effect of La_2O_3 addition on the thermal stability of γ-Al_2O_3 gels”. *Ceram Int* 30: 163-170.

[11] Johnson M. (1990) “Surface area stability of aluminas”. *J. Cat* 123: 245-259.

[12] Ozawa M, Kimura M. (1990). “Thermal stability and microstructure of catalytic alumina composite support with lanthanum species” *Mat. Sci. Lett.* 9: 291-293.

[13] Béguin B, Garbowski E, Primet M. (1991). “Stabilization of alumina by addition of lanthanum”. *J. Cat* 127: 595-604.

[14] Bettman M. (1989). "Alumina-based perovskite catalysts and catalysts supports*". J. Cat* 117: 447-454.

[15] Ferrer V., Finol D., González V., Espina F., Cauqui M., Dominguez F., (2015), "Comportamiento redox y actividad catalítica de óxidos mixtos basados en CeO2 soportados sobre La_2O_3-Al_2O_3", *Avances en Química*, 10: 83-92

[16] Rouquerol F., Rouquerol J., Sing K., Llewellyn P. Maurin G. (2014) "Adsorption by Powders and Porous Solids", Elsevier, Second edition, Oxford, UK.

[17] Sing K., Everett D., Haul R, Moscou L., Pierotti R., Rouquerol J., Siemieniewska T. (1985). "Reporting physisorption data for gas/solid systems with special reference to the determination of surface area and porosity (Recommendations 1984)", *Pure Appl Chem* 57: 603-619.

[18] Ersoy B, Gunay V. (2004) "Effect of La_2O_3 addition on the thermal stability of γ-Al_2O_3 gels" *Ceram Int.* 30: 163-170.

[19] Ismagilov Z, Shkrabina R, Koryabki N, Kapteijn F. (1995) "Synthesis of mechanically strong and thermally stable spherical alumina catalyst supports for the process of methane dimerization in a fluidized bed" *Catal. today* 24: 269-271.

[20] Doroftei C, Popa P, Iacomi F. (2012) "Synthesis of nanocrystalline La-Pb-Ce-Fe-O perovskite and methanol-sensing characteristics" *Sensor Actuat B-*Chem. 161: 977 - 981.

[21] Carter C.B., Norton M. G. (2013) "Ceramic Materials. Science and Engineering" Springer, Second edition.